UDC 519.632.4

ROBUST MILTIGRID TECHNIQUE FOR SOLVING PARTIAL DIFFERENTIAL EQUATIONS ON STRUCTURED GRIDS

S. I. Martynenko[1]

A new robust multigrid technique for solving elliptic partial differential equations is proposed. The technique is based on a united computational algorithm that consists of the following stages: 1) adaption of equations to numerical methods, 2) the control volume discretization, and 3) applying multigrid iterations. Special subgrids of the finest grid are generated to obtain the most powerful coarse grid correction strategy. Accuracy of the transfer operators is independent of the mesh size on coarse grids; therefore, a smoothing procedure and a multigrid cycle may be very simple. Expanded robustness of the multigrid technique is a result of adaption of equations, extremely accurate formulation of the discrete problems on the coarse grids, original coarsening, the most powerful coarse grid correction strategy, construction of problem-independent transfer operators, and absence of pre-smoothing and interpolation. The paper represents the algorithm, estimates of computational work, and results of numerical tests performed. Our numerical tests demonstrate robustness and efficiency of the multigrid technique.

1. Introduction. Iterative methods are often used to solve partial differential equations. As a rule, iterative methods should be adapted to a given problem. As a result, each fast solver includes some problem-dependent components (for example, an extrapolation factor in SOR, transfer operators and smoothing procedure in classical multigrid methods [1], a preconditioner in conjugate-gradient-like algorithms, etc.). Many iterative methods have been developed in recent years, and it is difficult to perform their comparison in detail. Unfortunately, a method that works well for one problem type may not work as well for another. Indeed, it may not work at all.

An iteration is called a robust one if it works for a sufficiently large class of problems [2]. We follow the point of view that a true robust solver should be based on *the adaption of problems to a computational algorithm*. Simple problems require trivial (problem-independent) modifications, and there is no drastic difference between original and adapted problems. However, complicated problems require problem-dependent modifications for the succeeding use of numerical methods. For example, the Navier–Stokes equations should be modified in order to obtain a strong coupling between velocity components and pressure. Adaption of problems to the computational algorithm can yield a single code to handle all modified problems.

Classical multigrid methods (C_MM) are known as very fast solvers for discretized partial differential equations [2]. In the first multigrid publication [3], R. P. Fedorenko formulated a multigrid algorithm for the standard five-point finite difference discretization of the Poisson equation on a square, proving that the work required to reach a given precision is $O(\tilde{N})$. In recent years, several pseudo-robust variants of C_MM have been proposed. We proceed from the assumption that the robust multigrid technique (R_MT) should be based on the following components:

1. *adaption of problems to a multigrid solver*. This adaption allows us to derive problem-independent computational part of R_MT;

2. *multiple coarse grid correction*. The use of extra coarse grids make the task of the smoother less demanding;

3. *vertex-and-cell-centered coarsening*. The advantage of the coarsening is that the transfer operators are problem-independent. What this means will be made clear in the sequel;

4. *control volume discretization*. Control volume discretization is more accurate than finite difference discretization for interface problems and lends itself to direct physical interpretation.

[1] Central Institute of Aviation Motors, Aviamotornaya 2, 111250 Moscow, Russian Federation, e-mail: martyn_s@mail.ru

This paper is concerned with the development of a single multigrid algorithm to handle all modified elliptic PDEs on structured grids.

2. Multigrid structure. For simplicity, let us consider a one-dimensional problem and assume that a uniform finest grid has been generated in the domain $\Omega = [0, 1]$. The computational grid $G(0;1)$ for the control volume discretization consists of two sets of grid points $G^{\rm v}(0;1)$ and $G^{\rm f}(0;1)$:

$$G^{\rm v}(0;1) = \{x_i^{\rm v} : x_i^{\rm v} = \Delta(i-1),\ \ i = 1, \ldots, {\rm H}_0 + 1,\ \ \Delta = {\rm H}_0{}^{-1}\}$$
$$G^{\rm f}(0;1) = \{x_i^{\rm f} : x_i^{\rm f} = 0.5\,(x_i^{\rm v} + x_{i+1}^{\rm v}),\ \ i = 1, \ldots, {\rm H}_0\}$$

The finest grid $G(0;1)$ can be represented as a union of three coarse grids $G(1;1)$, $G(1;2)$, and $G(1;3)$. Require that all these coarse grids have no common points and each coarse grid point coincides with a unique finest grid point:

$$G(0;1) = \bigcup_{k=1}^{3} G(1;k) \quad \text{and} \quad G(1;n) \cap G(1;m) = \emptyset\,, \quad n \neq m$$

The finest grid $G(0;1)$ forms the zero level and the three coarse grids $G(1;1)$, $G(1;2)$, and $G(1;3)$ form the first level. The coarse grid generation is further recurrently repeated: each grid $G(L;k)$, $k = 1, \ldots, 3^L$, of a current level L is considered to be the finest grid for the coarse grids $G(L+1;j)$, $j = 1, \ldots, 3^{L+1}$, of the next level $L+1$. The nine coarse grids derived from the three grids of the first level form the second level, etc. The coarse grid generation is finished when no further coarsening can be performed. It is clear that the finest grid can be represented as the following union of all grids of each level L:

$$G(0;1) = \bigcup_{k=1}^{3^L} G(L;k) \quad \text{and} \quad G(L;n) \cap G(L;m) = \emptyset\,, \quad n \neq m, \quad L = 1, \ldots, L^+$$

Here L^+ is the number of the coarsest level. An example of the coarse grid generation is shown in Figure 1. In what follows, the union of the finest grid and coarse grids will be called *the multigrid structure* (Figure 2).

Each grid of the multigrid structure has virtual grid points. Grids of the coarsest level have two virtual grid points; therefore, the number of virtual points on some grid of the Lth level is $2 \cdot 3^{L^+ - L}$. These virtual grid points are intended for computation of a restriction operator of RMT (Section 5).

The vertex-and-cell-centered coarsening used in RMT consists of deleting two grid points from each sets $G^{\rm v}$ and $G^{\rm f}$ as shown in Figure 3. The mesh-size on a coarse grid of the Lth level is $\Delta 3^L$, where Δ is the mesh-size on the uniform finest grid $G(0;1)$.

Assignment of a solution to the grid points $x^{\rm v}$ or $x^{\rm f}$ results in the vertex-centered discretization or cell-centered discretization. Control volumes on the finest grid are defined as $[x_{i-1}^{\rm f}, x_i^{\rm f}]$ and $[x_i^{\rm v}, x_{i+1}^{\rm v}]$, respectively. Note that a control volume on a coarse grid $G(L;k)$, $k = 1, \ldots, 3^L$, is a union of 3^L control volumes on the finest grid. Both these discretizations are not considered separately in RMT.

Actually, the notion "a grid of the Lth level" means the one-to-one mapping of indices of the coarse grid points onto the indices of the finest grid points. In what follows, the mapping will be denoted by the braces $\{\}$. For example, the mapping of indices of the grid points from the set $G^{\rm v}(1;1)$ will be written down as $x_{\{i\}}^{\rm v}$, where i and $\{i\}$ are the coarse and finest grid indices, respectively: $\{1\} = 3$; $\{2\} = 6$; $\{3\} = 9$; ... (Figure 1). The mapping of indices yields a close-to-the-finest-grid notation. In this case, the second order derivative can be approximated as

$$\left.\frac{\partial^2 u}{\partial x^2}\right|_{x_{\{i\}}^{\rm v}} = \frac{u_{\{i-1\}} - 2u_{\{i\}} + u_{\{i+1\}}}{\Delta^2 3^{2L}} + o(\Delta^2 3^{2L})$$

Figure 1 shows that the approximation of this derivative at the grid points $x_{\{2\}}^{\rm v} \in G^{\rm v}(1;1)$ is expressed as

$$\left.\frac{\partial^2 u}{\partial x^2}\right|_{x_{\{2\}}^{\rm v}} \approx \frac{u_{\{1\}} - 2u_{\{2\}} + u_{\{3\}}}{\Delta^2 3^2}, \qquad \text{what really means} \qquad \frac{u_3 - 2u_6 + u_9}{\Delta^2 3^2}$$

Coarse grids for solving N-dimensional problems are generated in each space coordinate. Each level consists of 3^{NL} coarse grids. The control volume on a coarse grid is a union of 3^{NL} control volumes of the finest grid.

3. Description of the robust multigrid technique. For simplicity, let us consider the one-dimensional problem

$$\frac{d^2 f}{dx^2} = 10\, e^x\,, \qquad f(0) = f(1) = 0 \tag{1}$$

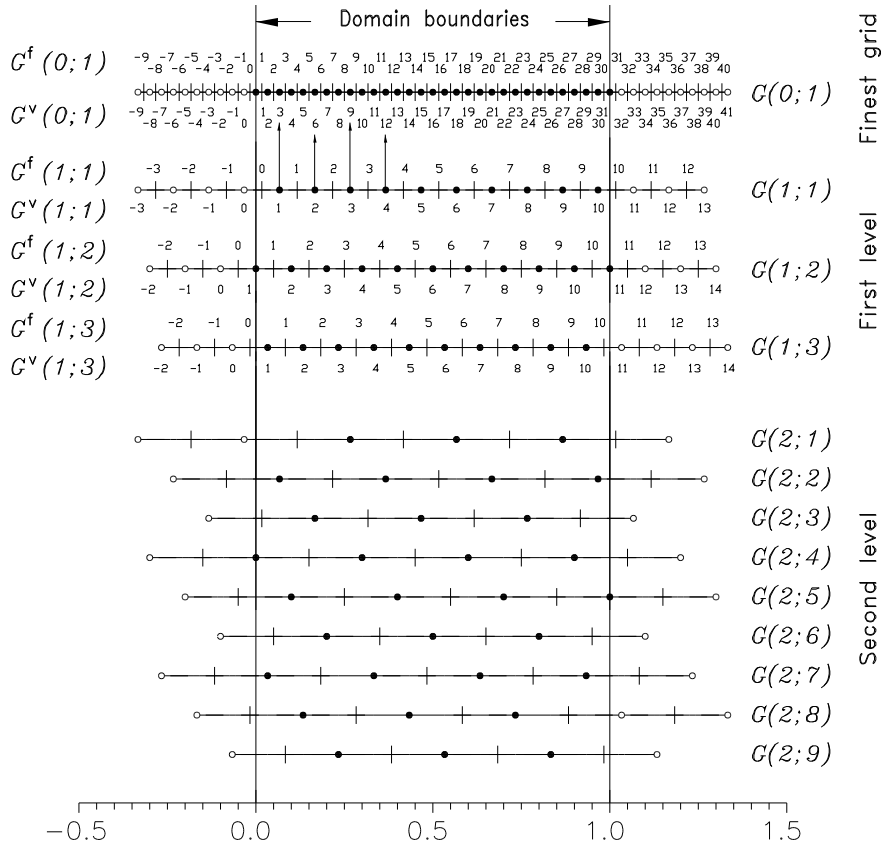

Fig. 1. Finest and coarse grids

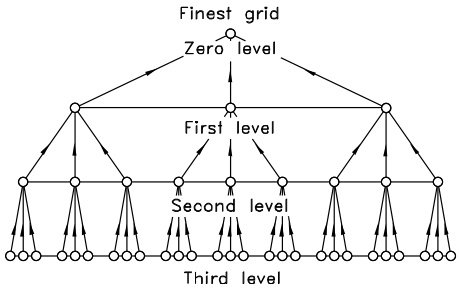

Fig. 2. Multigrid structure

in $\Omega = (0, 1)$. The exact solution of the problem is

$$f(\varrho) = 10\big(e^{\varrho} + (1 - e)\varrho - 1\big) \tag{2}$$

Before discretization, according to our approach, all problems to be solved should be modified into those acceptable for RMT. The solution f of (1) may be represented as

$$f = c + \hat{f} \tag{3}$$

The function $\hat{f}$ will be an approximation to the solution f and the function c will be a correction in the succeeding multigrid iterations. Representation (3) is called *the* Σ*-modification of a solution.* Substitution of (3) into (1) yields the following Σ*-modified form* of (1):

$$\frac{d^2c}{dx^2} = 10\,e^x - \frac{d^2\hat{f}}{dx^2}, \qquad c\big|_{\partial\Omega} = -\hat{f}\big|_{\partial\Omega} \tag{4}$$

The Σ-modification is one of the possible ways for the adaption of (1) to RMT.

Assume that a uniform computational grid has been generated and the function f is assigned to the grid points x^v. For a given PDE (or a system of PDEs), the required discretization (or grid) equations can be derived

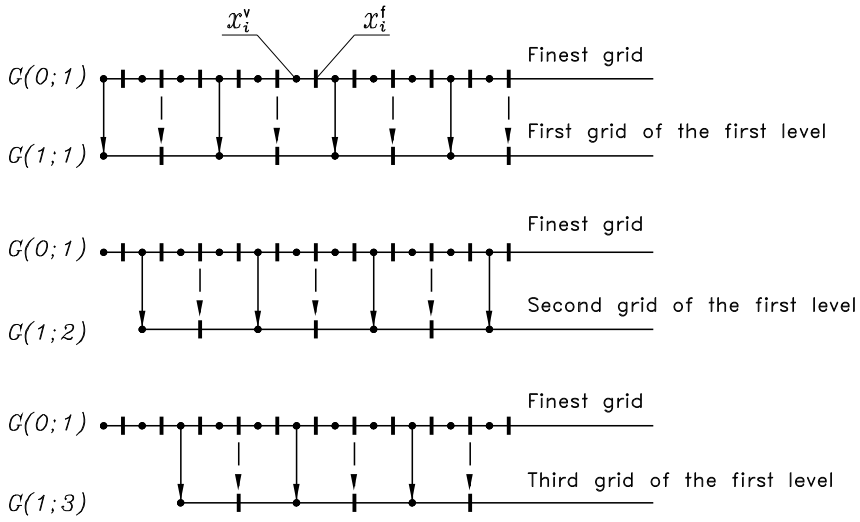

Fig. 3. Vertex-and-cell-centered coarsening in one dimension

in many ways. The control volume discretization is in most common use [4]. The computational domain is divided into a number of nonoverlapping control volumes such that there is one control volume which surrounds each grid point. The differential equation is integrated over each control volume. The most attractive feature of control volume discretization is that the resulting solution would satisfy the integral conservation laws over any group of control volumes. In addition, the control volume discretization is more accurate than the finite-difference discretization for interface problems [2]. Integration of (4) over the control volume $[x^{\mathrm{f}}_{\{i-1\}}, x^{\mathrm{f}}_{\{i\}}]$ yields the following finite-difference scheme:

$$\frac{c_{\{i-1\}} - 2c_{\{i\}} + c_{\{i+1\}}}{\Delta^2 3^{2L}} = J_{\{i\}}\,, \qquad \text{where} \qquad J_{\{i\}} = \frac{1}{\Delta 3^L} \int\limits_{x^{\mathrm{f}}_{\{i-1\}}}^{x^{\mathrm{f}}_{\{i\}}} \left(10\, e^x - \frac{d^2 \hat{f}}{dx^2}\right) dx \tag{5}$$

The values of c at the grid points outside the domain Ω can be eliminated by the following interpolation formulas:
a) the Dirichlet boundary condition at $x = 0$:

$$c_{\{0\}} = \frac{2}{\xi(\xi+1)}\; c|_{x=0} + 2\,\frac{\xi-1}{\xi}\, c_{\{1\}} - \frac{\xi-1}{\xi+1}\, c_{\{2\}} + o(\Delta^3 3^{3L}) \tag{6}$$

b) the Neumann boundary condition at $x = 0$:

$$c_{\{0\}} = -\frac{2\Delta 3^L}{2\xi+1}\; \frac{dc}{dx}\bigg|_{x=0} + 4\,\frac{\xi}{2\xi+1}\, c_{\{1\}} - \frac{2\xi-1}{2\xi+1}\, c_{\{2\}} + o(\Delta^3 3^{3L}) \tag{7}$$

c) the Dirichlet boundary condition at $x = 1$:

$$c_{\{\mathrm{H}_L+2\}} = \frac{2}{\xi(\xi+1)}\; c|_{x=1} + 2\,\frac{\xi-1}{\xi}\, c_{\{\mathrm{H}_L+1\}} - \frac{\xi-1}{\xi+1}\, c_{\{\mathrm{H}_L\}} + o(\Delta^3 3^{3L}) \tag{8}$$

d) the Neumann boundary condition at $x = 1$:

$$c_{\{\mathrm{H}_L+2\}} = \frac{2\Delta 3^L}{2\xi+1}\; \frac{dc}{dx}\bigg|_{x=1} + 4\,\frac{\xi}{2\xi+1}\, c_{\{\mathrm{H}_L+1\}} - \frac{2\xi-1}{2\xi+1}\, c_{\{\mathrm{H}_L\}} + o(\Delta^3 3^{3L}) \tag{9}$$

Here

$$\xi = \begin{cases} \dfrac{x^{\mathrm{v}}_{\{1\}}}{\Delta 3^L}\,, & x = 0 \\[2ex] \dfrac{1 - x^{\mathrm{v}}_{\{\mathrm{H}_L+1\}}}{\Delta 3^L}\,, & x = 1 \end{cases}$$

As an example, we consider the three-level algorithm. The grids of the multigrid structure are visited in a sawtooth-cycle manner. The sawtooth cycle is a special case of the V-cycle in which smoothing before coarse

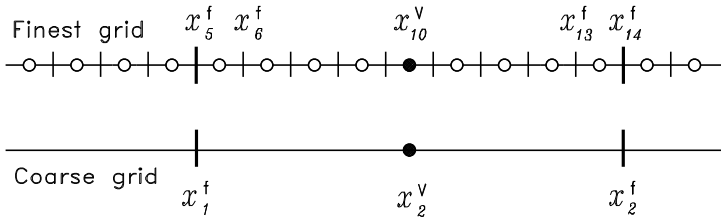

Fig. 4. Points of some coarse grid of the second level

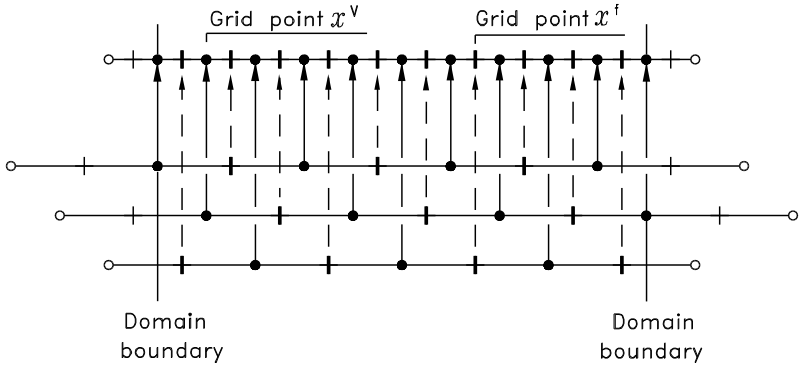

Fig. 5. The injection operator

grid correction (pre-smoothing) is deleted [2]. Iterations start from the coarsest level (Figure 2). Consider some grid of this level (Figure 4). The integrals $J_{\{i\}}$ in the right-hand side of (5) should be computed before the smoothing iterations. Since the control volume $[x^{\mathrm{f}}_{\{1\}}, x^{\mathrm{f}}_{\{2\}}]$ of the coarse grid is a union of the nine control volumes on the finest grid

$$[x^{\mathrm{f}}_{\{1\}}, x^{\mathrm{f}}_{\{2\}}] \equiv [x^{\mathrm{f}}_5, x^{\mathrm{f}}_{14}] = [x^{\mathrm{f}}_5, x^{\mathrm{f}}_6] \cup [x^{\mathrm{f}}_6, x^{\mathrm{f}}_7] \cup \cdots \cup [x^{\mathrm{f}}_{12}, x^{\mathrm{f}}_{13}] \cup [x^{\mathrm{f}}_{13}, x^{\mathrm{f}}_{14}]$$

the integral $J_{\{2\}}$ can be computed as

$$J^{L=2}_{\{2\}} = \frac{1}{\Delta\, 3^2}\left[\int\limits_{x^{\mathrm{f}}_5}^{x^{\mathrm{f}}_6} \left(10\, e^x - \frac{d^2 \hat{f}}{dx^2}\right) dx + \cdots + \int\limits_{x^{\mathrm{f}}_{13}}^{x^{\mathrm{f}}_{14}} \left(10\, e^x - \frac{d^2 \hat{f}}{dx^2}\right) dx \right]$$

Let us denote

$$R^{\star}_m = \frac{1}{\Delta} \int\limits_{x^{\mathrm{f}}_{m-1}}^{x^{\mathrm{f}}_m} \left(10\, e^x - \frac{d^2 \hat{f}}{dx^2}\right) dx = 10\, e^{x^{\mathrm{v}}_m} - \frac{\hat{f}_{m-1} - 2\hat{f}_m + \hat{f}_{m+1}}{\Delta^2} + o(\Delta^2)$$

It is clear that the integrals $R^{\star}_m$ are residuals of the discretization equation computed on the finest grid. Thus, the integral $J_{\{2\}}$ can be rewritten as

$$J^{L=2}_{\{2\}} = \frac{1}{3^2}\left(R^{\star}_6 + \cdots + R^{\star}_{14}\right) + o(\Delta^2)$$

It is easy to see that the integral J is the arithmetic mean value of residuals computed at the finest grid points $x^{\mathrm{v}}_i \in [x^{\mathrm{f}}_{\{1\}}, x^{\mathrm{f}}_{\{2\}}]$. The integral J is a restriction operator of RMT. Since the integrals $J_{\{i\}}$ are computed on the finest grid, accuracy of the computations is independent of the mesh size on coarse grids. Generally, the restriction operator uses 3^{NL} finest grid points for averaging the residual on grids of the Lth level. The three-level algorithm is considered here only to emphasize the feature of the restriction operator.

Similar computations (evaluation of the integrals and post-smoothing) are performed on each grid of the coarsest level (Figure 2). When the coarsest level solution has been obtained, the transfer to the next finer level is performed as shown in Figure 5. It should be noted that the transfer does not add any interpolation errors in

Table 1. Evolution of error in RMT (left) and CMM (right)

Level	Grid	Error E	Grid	Error E
—	—	$2.12 \cdot 10^{+0}$	—	$2.12 \cdot 10^{+0}$
1	1	$2.17 \cdot 10^{-2}$	1	$3.48 \cdot 10^{-3}$
1	2	$4.49 \cdot 10^{-3}$	—	—
1	3	$9.41 \cdot 10^{-3}$	—	—
0	1	$3.84 \cdot 10^{-3}$	1	$5.03 \cdot 10^{-2}$

the correction c, since all coarse grids are subgrids of the finest grid (Figure 1). The transfer is a prolongation (injection) operator of RMT.

Smooth parts of the error are deleted on all grids of the next finer levels in a similar manner (i.e., computation of the integral J and the use of smoothing iterations). The restriction operator on the first level is defined by

$$J_{\{i\}}^{L=1} = \frac{1}{3}\left(R_{\{i\}-1}^{\star} + R_{\{i\}}^{\star} + R_{\{i\}+1}^{\star}\right) + o(\Delta^2)$$

The coarse grid correction to be added to $\hat{f}$ on the finest grid is c ($\hat{f} := \hat{f} + c$). The multigrid iterations repeatedly improve the approximate solution $\hat{f}$ until the current approximation becomes accurate enough.

To illustrate RMT in the step-by-step manner, we solve (1) with a uniform grid ($\Delta = \mathrm{H}_0{}^{-1} = 0.1$, two level structure: $L^+ = 1$), starting iterand zero. Let us consider only the first multigrid iteration. Computations start from the first grid of the first level: $\{1\} = 3$, $\{2\} = 6$, $\{3\} = 9$ (Figure 6). Next, the discretization equation is solved on the second grid ($\{1\} = 1$, $\{2\} = 4$, $\{3\} = 7$, $\{4\} = 10$) of the first level. Finally, the discretization equation is solved on the third grid ($\{1\} = 2$, $\{2\} = 5$, $\{3\} = 8$, $\{4\} = 11$) of the first level. All numerical solutions are shown in Figure 6. The next step of RMT includes the transfer to the finest grid. Actually, the transfer consists in the change of the one-to-one mapping of indices: $\{i\} \equiv i$. Three Gauss–Seidel iterations ($\nu = 3$) are performed on the finest grid to delete rough parts of the error. In order to estimate the efficiency of RMT, we define an error of the numerical solution as follows: $\mathrm{E} = \max_{\{i\}} |f(x_{\{i\}}^{\mathrm{v}}) - c_{\{i\}}|$. Here f is the exact solution given by (2). Evolution of the error is shown in Table 1. The first row of the table corresponds to the starting guess.

In addition, we solve (1) by CMM (the sawtooth cycle and linear interpolation). The numerical results obtained are shown in Figure 6 and Table 1.

Our numerical experiments showed that it is very difficult to compare the convergence rates of RMT and CMM. On the one hand, RMT approximates the long wavelength parts of the error on coarser grids more accurately than CMM. It is expected that RMT requires the least number of the multigrid iterations to obtain a numerical solution. In general, RMT uses the least number of levels to compute the correction c. On the other hand, computational cost of the robust multigrid iterations is higher than that of the classical iterations. Note that the comparison between RMT and CMM is problem-dependent.

4. Advantages of the robust multigrid technique. Let us summarize the advantages of RMT over CMM and clarify some details of the technique.

1. *Extremely accurate formulation of discrete problems on coarse grids.* As an example, we consider the two-dimensional problem

$$\frac{\partial^2 u}{\partial x^2} + \frac{\partial^2 u}{\partial y^2} + \gamma(x,y)\, u = F(x,y)\,, \quad u|_{\partial\Omega} = g$$

in $\Omega = (0,1) \times (0,1)$. This problem can be rewritten in the Σ-modified form as follows:

$$\frac{\partial^2 c}{\partial x^2} + \frac{\partial^2 c}{\partial y^2} + \gamma(x,y)\, c = r(x,y)\,, \quad c|_{\partial\Omega} = g - \hat{u}|_{\partial\Omega}$$

Here

$$r(x,y) = F(x,y) - \frac{\partial^2 \hat{u}}{\partial x^2} - \frac{\partial^2 \hat{u}}{\partial y^2} - \gamma(x,y)\, \hat{u}$$

Assume that the functions $\hat{u}$ and c are assigned to the grid points $(x^{\mathrm{v}}, y^{\mathrm{v}})$. Integration of the above Σ-modified equation over a control volume $\bar{\Omega}_{\{ij\}}$

$$\bar{\Omega}_{\{ij\}} = \left\{(x,y) \mid x_{\{i-1\}}^{\mathrm{f}} \leqslant x \leqslant x_{\{i\}}^{\mathrm{f}}, y_{\{j-1\}}^{\mathrm{f}} \leqslant y \leqslant y_{\{j\}}^{\mathrm{f}}\right\} \tag{10}$$

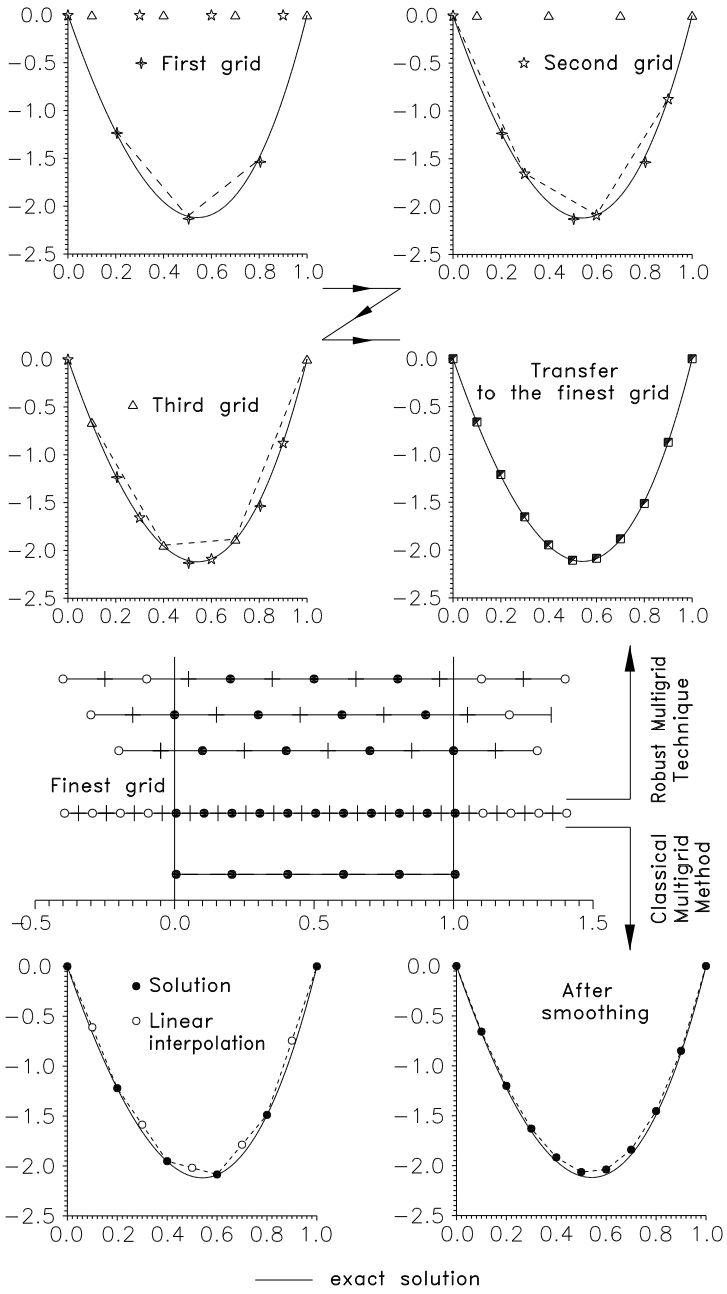

Fig. 6. Comparison of the robust multigrid technique and classical multigrid method

yields the following finite-difference scheme:

$$\frac{c_{\{i-1j\}} - 2c_{\{ij\}} + c_{\{i+1j\}}}{\Delta^2 3^{2L}} + \frac{c_{\{ij-1\}} - 2c_{\{ij\}} + c_{\{ij+1\}}}{\Delta^2 3^{2L}} + \langle\gamma\rangle_{\{ij\}} c_{\{ij\}} = J_{\{ij\}}$$

Here

$$\langle\gamma\rangle_{\{ij\}} = \frac{1}{\Delta^2 3^{2L}} \int\limits_{x^{\mathrm{f}}_{\{i-1\}}}^{x^{\mathrm{f}}_{\{i\}}} \int\limits_{y^{\mathrm{f}}_{\{j-1\}}}^{y^{\mathrm{f}}_{\{j\}}} \gamma(x,y)\, dy\, dx \tag{11}$$

In order to formulate the discrete problems with extreme accuracy on coarse grids, the integral J and the coefficient $\langle\gamma\rangle$ must be computed on the finest grid. This allows us to decrease the order of approximation down to $o(\Delta^2)$. The resulting linear system may be abbreviated as

$$A\boldsymbol{x} = \boldsymbol{b}$$

In fact, we have a perturbed system

$$(A + \delta_A)(\boldsymbol{x} + \boldsymbol{\delta_x}) = (\boldsymbol{b} + \boldsymbol{\delta_b})$$

where the errors of the coefficient matrix (δ_A) and right-hand side vector ($\boldsymbol{\delta_b}$) result in an error ($\boldsymbol{\delta_x}$) of the solution. Accurate computations of the coefficient $\langle\gamma\rangle$ and integral J minimize the errors δ_A and $\boldsymbol{\delta_b}$, and, hence, $\boldsymbol{\delta_x}$. Accuracy of the correction c depends only on the number of smoothing iterations and the mesh size on a given grid.

Now we explain the Σ-modification of PDEs. At first, recall a similar procedure in C$_{\text{M}}$M [2]. Let us consider a linear problem

$$\mathcal{L}(u) = f\,, \qquad u|_{\partial\Omega} = g \tag{12}$$

where $\mathcal{L}$ is some linear differential operator. Problem (12) can be discretized using finite differences. The resulting discretization equations are written down as

$$A\boldsymbol{u} = \boldsymbol{b} \tag{13}$$

Let $\hat{\boldsymbol{u}}$ be an approximation to the solution of (13). The error $\boldsymbol{e} \equiv \hat{\boldsymbol{u}} - \boldsymbol{u}$ is to be approximated on the coarse grid. We have

$$A\boldsymbol{e} = -\boldsymbol{r} \equiv A\hat{\boldsymbol{u}} - \boldsymbol{b}$$

The coarse grid approximation $\bar{\boldsymbol{u}}$ of $-\boldsymbol{e}$ satisfies

$$A\bar{\boldsymbol{u}} = R\boldsymbol{r} \tag{14}$$

where R is a problem-dependent restriction operator of C$_{\text{M}}$M. In the two-level algorithm it is assumed that (14) is solved exactly. The coarse grid correction to be added to $\hat{\boldsymbol{u}}$ is $P\bar{\boldsymbol{u}}$:

$$\hat{\boldsymbol{u}} := \hat{\boldsymbol{u}} + P\bar{\boldsymbol{u}}$$

Here P is a problem-dependent prolongation operator of C$_{\text{M}}$M.

Contrary to C$_{\text{M}}$M [1], R$_{\text{M}}$T can be understood as a fixed algorithm that consists of the following steps.

Step 1: *Adaption of problem* (12) *to* R$_{\text{M}}$T. The linear problem can be rewritten in the Σ-modified form as

$$\mathcal{L}(c) = f - \mathcal{L}(\hat{u})\,, \qquad c|_{\partial\Omega} = g - \hat{u}|_{\partial\Omega}$$

Step 2: *Generation of the multigrid structure.*

Step 3: *Control volume discretization of the modified problem.* Integration of the Σ-modified problem over a control volume V_g^L on some computational grid g of the Lth level yields

$$\frac{1}{V_g^L}\int\limits_{V_g^L} \mathcal{L}(c)\,dv = J\,, \qquad \text{where} \qquad J = \frac{1}{V_g^L}\int\limits_{V_g^L} \bigl(f - \mathcal{L}(\hat{u})\bigr)\,dv$$

The integral J is similar to $\mathbf{Rr}$ in C$_{\text{M}}$M. The discretization equations can be written as

$$\bar{A}c = J$$

Step 4: *Multigrid iterations* (the sawtooth cycle). The coarse grid correction to be added to $\hat{u}$ is c:

$$\hat{u} := \hat{u} + c$$

At first glance, the Σ-modification $u = \hat{u} + c$ in R$_{\text{M}}$T is similar to $\boldsymbol{u} = \hat{\boldsymbol{u}} - \boldsymbol{e}$ in C$_{\text{M}}$M, but it is this combination of such adaption of problems, original coarsening and control volume discretization that yields the extremely accurate formulation of discrete problems on coarse grids. As a result, this accurate formulation makes it possible to avoid the necessity of pre-smoothing in the multigrid iterations. Another variant of adaption of problems to R$_{\text{M}}$T (so-called Π-modification) will be discussed in Subsection 7.4. Actually, the adaption of problems is the only problem-dependent component of R$_{\text{M}}$T.

2. *Improvement of numerical solutions.* It is desirable that the coefficient matrix of the resulting linear system be an M-matrix [2]. In order to obtain an M-matrix in applications of computational fluid dynamics (CFD), the first derivatives in momentum or transport equations are often discretized by upwind discretization.

However, the upwind discretization reduces the approximation order. To illustrate this difficulty, consider the one-dimensional convection-diffusion equation

$$\frac{du}{dx} + \varepsilon \frac{d^2u}{dx^2} = 0$$

The representation of the first derivative by means of central difference leads to the following finite-difference scheme

$$\frac{u_{i+1} - u_{i-1}}{2\Delta} + \varepsilon \frac{u_{i+1} - 2u_i + u_{i-1}}{\Delta^2} = 0$$

This scheme has the second approximation order $o(\Delta^2)$; however, to obtain an M-matrix, the computational grid should satisfy the condition $\Delta < 2\varepsilon$. On the other hand, the representation of the first derivative by the upwind difference allows us to obtain the M-matrix

$$\frac{u_{i+1} - u_i}{\Delta} + \varepsilon \frac{u_{i+1} - 2u_i + u_{i-1}}{\Delta^2} = 0$$

However, the upwind discretization reduces the approximation order down to $o(\Delta)$. In classical solvers, the discretization equations can be modified to increase the approximation order. It is clear that the scheme

$$\frac{u_{i+1}^{n+1} - u_i^{n+1}}{\Delta} + \varepsilon \frac{u_{i+1}^{n+1} - 2u_i^{n+1} + u_{i-1}^{n+1}}{\Delta^2} = \frac{u_{i+1}^{n} - u_i^{n}}{\Delta} - \frac{u_{i+1}^{n} - u_{i-1}^{n}}{2\Delta}$$

yields the M-matrix and the second approximation order for a convergent solution. The equation adapted to RMT can be written as

$$\frac{1}{\Delta\, 3^L} \int\limits_{x^{\mathrm{f}}_{\{i-1\}}}^{x^{\mathrm{f}}_{\{i\}}} \left(\frac{dc}{dx} + \varepsilon \frac{d^2c}{dx^2} \right) dx = J_{\{i\}}\,, \qquad \text{where} \qquad r(x) = -\frac{d\hat{u}}{dx} - \varepsilon \frac{d^2\hat{u}}{dx^2}$$

Both sides of this equation may be discretized separately. The left-hand side of the equation is discretized by using the upwind difference to obtain the M-matrix as follows:

$$\frac{c_{\{i+1\}} - c_{\{i\}}}{\Delta 3^L} + \varepsilon \frac{c_{\{i+1\}} - 2c_{\{i\}} + c_{\{i-1\}}}{\Delta^2 3^{2L}} = J_{\{i\}}$$

The integral J should be computed on the finest grid to reach the second approximation order in a way that

$$R_m^{\star} = -\frac{\hat{u}_{m+1} - \hat{u}_{m-1}}{2\Delta} - \varepsilon \frac{\hat{u}_{m+1} - 2\hat{u}_m + \hat{u}_{m-1}}{\Delta^2} + o(\Delta^2)$$

It is easy to see that the convergent solution (i.e., $c = 0$) will have the second approximation order. In comparison with CMM, RMT does not require any artificial modification of the discretization equations to obtain a more accurate numerical solution. Instead, separate discretization of the left-hand side operator and right-hand side integral can be used to overcome the conflicting situations (for example, the M-matrix vs accuracy). It may be noted that for a single-grid solver ($\{i\} \equiv i$) the separate discretization is about equally efficient as the defect correction [5]. An example of application of the separate discretization to solve the Poisson equation will be given below (Test 2 in Subsection 7.1).

3. *Original coarsening.* Vertex-and-cell-centered coarsening used in RMT incorporates the advantages of vertex-centered and cell-centered coarsening. In addition, this coarsening reduces the number of levels without deterioration of convergence. The generation of the coarse grids in RMT is independent of location of control volumes on the finest grid. As opposed to CMM, the control volumes should be specified before discretization of PDEs on the multigrid structure.

4. *Incorporation of the control volume discretization and multigrid iterations.* This incorporation simplifies the development of an efficient multigrid solver for a large class of physically meaningful problems. In addition, the discretization admits a direct physical interpretation.

5. *Problem-independent transfer operators.* The proofs of mesh-size independent rate of convergence of CMM assume that the transfer operators satisfy a certain condition [2]. The transfer operators of RMT are independent of the smoothers, problems to be solved, unknown ordering, grid aspect ratio, etc. The most obvious example for illustration of the advantage of the prolongation operator is interface problems. Since the

linear interpolation across discontinuities is inaccurate, CMM requires the operator-dependent prolongation to handle these problems [6]. The absence of any interpolation in RMT results in the absence of such difficulties (Subsection 7.3).

6. *The most powerful coarse grid correction strategy.* The multigrid structure is an example of the most powerful coarse grid correction strategy where the most Fourier modes of the error are approximated on the coarse levels in order to make task of the smoother the least demanding. Moreover, the transfer operators do not contribute any error to the numerical solution.

7. *The simplest multigrid cycle.* RMT uses the simplest multigrid schedule (namely, the sawtooth cycle). Pre-smoothing in CMM leads to certain difficulties when solving nonlinear equations [2]. The absence of pre-smoothing in RMT results in the absence of such difficulties.

8. *Expanded robustness.* The expanded robustness of this multigrid technique is a result of adaption of equations, extremely accurate formulation of the discrete problems on the coarse grids, original coarsening, the most powerful coarse grid correction strategy, construction of problem-independent transfer operators, and absence of pre-smoothing and interpolation.

9. *Black box properties.* Since the main components of RMT (generation of the multigrid structure, one-to-one mapping of indices, and computation of integrals) are problem-independent, they can be realized as black box subroutines. In addition, discrete problems on the multigrid structure are specified in a close-to-the-finest-grid manner (for example, (5)). The introduction to the FORTRAN implementation will be given in [7]. The main difference between RMT and single-grid smoothers consists in the approximation of boundary conditions on coarse grids ((6) – (9)).

All numerical tests in this paper are performed without any change of components of RMT. We use Alternating Line Gauss-Seidel (ALGS) in the numerical experiments for simplicity of programming. Theoretical analysis shows that ALGS is found to be a robust smoother for many problems [2]. In addition, this smoother does not require a global linearization of the nonlinear discrete problems. For simplicity, it is assumed that the solution is assigned to the grid points $(x^{\mathrm{v}}, y^{\mathrm{v}})$. The point Gauss-Seidel smoother and staggered grids will be discussed in our following publications.

The only disadvantage of RMT consists in an increase of computational efforts per multigrid iteration as compared with CMM. This fact is discussed in Section 8.

5. Computation of integrals. Evaluation of integrals is the most important component of RMT. Their direct computation on the finest grid described in Section 3 requires excessive efforts. However, the properties of the coarse grid generation allow us to propose a fast method for evaluating integrals. Assume that the integrand $r(x)$ is defined to be zero outside the domain Ω. Let us define a characteristic function $\Upsilon(x)$ such that

$$\Upsilon(x) = \begin{cases} 0\,, & x \in \Omega \\ 1\,, & x \notin \Omega \end{cases}, \qquad \check{r}(x) = \begin{cases} 0\,, & x \in \Omega \\ r(x)\,, & x \notin \Omega \end{cases}$$

According to the above definitions, the integral J^L can be rewritten as

$$J^L_{\{i\}} = \frac{1}{\Delta\, 3^L} \int\limits_{x^{\mathrm{f}}_{\{i-1\}}}^{x^{\mathrm{f}}_{\{i\}}} r(x)\, dx = \frac{\hat{J}^L_{\{i\}}}{\Lambda^L_{\{i\}}} \tag{15}$$

where

$$\hat{J}^L_{\{i\}} = \frac{1}{\Delta} \int\limits_{x^{\mathrm{f}}_{\{i-1\}}}^{x^{\mathrm{f}}_{\{i\}}} \check{r}(x)\, dx \qquad \text{and} \qquad \Lambda^L_{\{i\}} = \frac{1}{\Delta} \int\limits_{x^{\mathrm{f}}_{\{i-1\}}}^{x^{\mathrm{f}}_{\{i\}}} \Upsilon(x)\, dx$$

Here $\Lambda^L_{\{i\}}$ is the number of actual control volumes on the finest grid that form the control volume on some grid. The evaluation of the integral J on the L^*th level starts from the finest grid. At this stage, we compute

$$J^{L=0}_m = \hat{J}^{L=0}_m = \frac{1}{\Delta} \int\limits_{x^{\mathrm{f}}_{m-1}}^{x^{\mathrm{f}}_m} r(x)\, dx\,, \qquad x^{\mathrm{v}}_m \in \Omega \qquad \text{and} \qquad \Lambda^{L=0}_m = \frac{1}{\Delta} \int\limits_{x^{\mathrm{f}}_{m-1}}^{x^{\mathrm{f}}_m} \Upsilon(x)\, dx = \begin{cases} 1\,, & x^{\mathrm{v}}_m \in \Omega \\ 0\,, & x^{\mathrm{v}}_m \notin \Omega \end{cases}$$

Since each control volume on a coarse grid of the Lth level is a union of the three control volumes on the finer grid of the $(L-1)$th level, the integrals $\hat{J}^L$ and Λ^L can be computed starting from the first level down to the

L^*th level by the following recurrence formulas:

$$\begin{cases} \hat{J}^L_{\{i\}} = \hat{J}^{L-1}_{\{i\}-3^{L-1}} + \hat{J}^{L-1}_{\{i\}} + \hat{J}^{L-1}_{\{i\}+3^{L-1}}, \\ \Lambda^L_{\{i\}} = \Lambda^{L-1}_{\{i\}-3^{L-1}} + \Lambda^{L-1}_{\{i\}} + \Lambda^{L-1}_{\{i\}+3^{L-1}}, \end{cases} \qquad L = 1, \ldots, L^*$$

Finally, the integral J^{L^*} on the L^*th level is computed as was done for (15). We used $2 \cdot 3^{L^+-L}$ virtual grid points only for the above evaluations of the integrals.

Multidimensional integrals can be computed as iterated one-dimensional integrals. Let us define one work unit (WU$\{0\}$) as the amount of computing work required for the computation of the integral J on the finest grid. The total amount of the work for evaluation of N-dimensional integrals on all grids of the Lth level is given by

$$\mathrm{WU}_\Sigma\{L\} = \mathrm{WU}\{0\} + \varpi\bar{\mathbf{N}}L \quad \text{f.p.o.}$$

(floating point operations), where $\varpi = 2 \cdot 3^N - 1$ and $\bar{\mathbf{N}}$ is the number of the finest grid points. Assume that

- the coarsest grids have 3^N points: $\bar{\mathbf{N}} = 3^{N(L^+ + 1)} \Rightarrow L^+ = \dfrac{1}{N}\dfrac{\lg \bar{\mathbf{N}}}{\lg 3} - 1$
- amount of the work for calculation of integrals on the finest grid is proportional to the number of grid points: $\mathrm{WU}\{0\} = C_I\bar{\mathbf{N}}$, where C_I is a problem-dependent constant.

In a large memory computing (LMC), the integrals are computed only once on each level before the use of each multigrid iteration, and their values are stored in the core memory. In this case, the total work can be estimated as

$$\mathrm{WU}_\Sigma = \mathrm{WU}\{0\} + \varpi\bar{\mathbf{N}}L^+ = \bar{\mathbf{N}}\left(C_I + \frac{\varpi}{N}\frac{\lg \bar{\mathbf{N}}}{\lg 3} - \varpi\right) \quad \text{f.p.o.}$$

LMC requires extra computer memory for storage of $\bar{\mathbf{N}}L^+$ single precision numbers (`Real * 4`).

In a small memory computing (SMC), the integrals are computed on each level before the use of the smoothing iterations and, their values are not stored in the core memory; therefore,

$$\mathrm{WU}_\Sigma = \sum_{l=0}^{L^+} \mathrm{WU}\{0\} + \varpi\bar{\mathbf{N}}\sum_{l=1}^{L^+} l = \frac{\bar{\mathbf{N}}}{N}\frac{\lg \bar{\mathbf{N}}}{\lg 3}\left(C_I + \frac{\varpi}{2N}\frac{\lg \bar{\mathbf{N}}}{\lg 3} - \frac{\varpi}{2}\right) \text{ f.p.o.}$$

Thus, the total amount of work for computation of the integral has the following asymptotic behavior:

$$\mathrm{WU}_\Sigma = \begin{cases} O(\bar{\mathbf{N}} \lg \bar{\mathbf{N}}) & - \text{ large memory computing (LMC)}, \\ O(\bar{\mathbf{N}} \lg^2 \bar{\mathbf{N}}) & - \text{ small memory computing (SMC)}, \\ O(\bar{\mathbf{N}}^{\mathbf{2}}) & - \text{ direct computing}, \end{cases} \qquad \text{as} \qquad \bar{\mathbf{N}} \to +\infty$$

6. Computational work. Let us introduce the concept of *equivalent number of iterations*. Assume that $\nu\{L; g\}$ iterations are performed on each grid g ($1 \leqslant g \leqslant 3^{NL}$) of the Lth level. The equivalent number of iterations is the following grid-averaged number:

$$\hat{\nu}\{L\} = \frac{1}{3^{NL}}\sum_{g=1}^{3^{NL}} \nu\{L; g\}$$

According to the main feature of the multigrid structure (the absence of common grid points on various grids of the same level), the computational efforts for $\hat{\nu}\{L\}$ iterations on all grids of the Lth level and on the finest grid are approximately the same. The concept of equivalent number of iterations makes it possible to compare the amount of computation on different levels. Following Brandt [8], one work unit is defined as the work involved in one smoothing iteration on the finest grid. For simplicity of theoretical analysis, assume that the same number ν of smoothing iterations is performed on each grid: $\hat{\nu}\{L\} = \nu$, $0 \leqslant L \leqslant L^+$. The computational work required for one equivalent iteration of ALGS is expressed as

$$\left.\begin{array}{ll} \text{2D problems:} & 2\mathrm{H}_0\,(8\mathrm{H}_0 - 6) \approx 16\bar{\mathbf{N}} \\ \text{3D problems:} & 6\mathrm{H}_0^2\,(8\mathrm{H}_0 - 6) \approx 48\bar{\mathbf{N}} \end{array}\right\} = 8N(N-1)\bar{\mathbf{N}} \quad \text{f.p.o.}$$

Table 2. Distribution of the computational efforts (LMC)

component	$\nu = 1$	$\nu = 2$	$\nu = 3$	$\nu = 4$	$\nu = 5$
the smoothing procedure (ALGS)	47.5%	64.4%	73.1%	78.4%	81.9%
the transfer operators	52.5%	35.6%	26.9%	21.6%	18.1%

Table 3. Comparison of LCM and SMC ($\nu = 3$)

$\bar{\mathbf{N}}$	10^3	10^4	10^5	10^6	10^7	10^8
2D problems	0.88	0.78	0.71	0.65	0.59	0.55
3D problems	1.00	0.92	0.84	0.78	0.73	0.69

where $\bar{\mathbf{N}} = (\mathrm{H}_0 + 1)^N \approx \Delta^{-N}$. The computational work required for the smoothing procedure can be estimated as

$$8N(N-1)\nu\bar{\mathbf{N}}(L^+ + 1) = \frac{8(N-1)\nu}{\lg 3}\,\bar{\mathbf{N}}\lg\bar{\mathbf{N}} \approx 16(N-1)\nu\,\bar{\mathbf{N}}\lg\bar{\mathbf{N}} \quad \text{f.p.o.}$$

Consider LMC and assume that $C_I = \varpi = 2 \cdot 3^N - 1$. The distribution of the computational efforts is given by

$$\begin{cases} \dfrac{2 \cdot 3^N - 1}{2 \cdot 3^N - 1 + 8(N-1)N\nu} \approx \dfrac{9}{9 + 8\nu} & - \text{ computation of the integrals} \\ \dfrac{8(N-1)N\nu}{2 \cdot 3^N - 1 + 8(N-1)N\nu} \approx \dfrac{8\nu}{9 + 8\nu} & - \text{ the smoothing procedure (ALGS)} \end{cases}$$

Table 2 reports the distribution as a function of the number ν of smoothing iterations.

Consider SMC and assume that $C_I = 0.5\,\varpi = 3^N - 0.5$. The distribution of the computational efforts is given by

$$\begin{cases} \dfrac{(2 \cdot 3^N - 1)\lg\bar{\mathbf{N}}}{(2 \cdot 3^N - 1)\lg\bar{\mathbf{N}} + 8(N-1)N^2\nu} & - \text{ computation of the integrals} \\ \dfrac{8(N-1)N^2\nu}{(2 \cdot 3^N - 1)\lg\bar{\mathbf{N}} + 8(N-1)N^2\nu} & - \text{ the smoothing procedure (ALGS)} \end{cases}$$

In order to estimate the influence of costs of SMC on the total work, assume that the computational efforts for the evaluation of the integrals are less or equal to the efforts for the smoothing procedure:

$$\frac{(2 \cdot 3^N - 1)\lg\bar{\mathbf{N}}}{(2 \cdot 3^N - 1)\lg\bar{\mathbf{N}} + 8(N-1)N^2\nu} \leqslant \frac{1}{2} \;\Rightarrow\; \lg\bar{\mathbf{N}} \leqslant 4(N-1)N^2\nu 3^{-N}$$

SMC of the restriction operator will be more effective for medium-size problems:

$$\bar{\mathbf{N}} \leqslant \begin{cases} 450 \times 450, & \text{2D problems} \\ 450 \times 450 \times 450, & \text{3D problems} \end{cases} \qquad \text{and} \quad \nu = 3$$

To compare the efficiency of the methods for computing the restriction operator, consider the ratio of the total efforts for LMC and SMC

$$\frac{\text{total efforts for LMC}}{\text{total efforts for SMC}} \approx \frac{3^N N + 4(N-1)N^2\nu}{3^N \lg\bar{\mathbf{N}} + 4(N-1)N^2\nu}$$

Table 3 represents this ratio. Of course, extra computer memory ($\bar{\mathbf{N}}L^+$ single precision numbers) in LMC leads to the reduction of computational time.

In general, the multigrid methods can solve many problems at a cost of $O(\bar{\mathbf{N}}\,\lg^k\bar{\mathbf{N}})$ f.p.o., where

$$k = \begin{cases} 0\,, & \text{classical multigrid methods} \\ 1\,, & \text{robust multigrid technique (LMC)} \\ 2\,, & \text{robust multigrid technique (SMC)} \end{cases}$$

7. Numerical experiments. Our $\mathrm{R_MT}$ consists of two parts: the analytical modification of the boundary value problems and the multigrid algorithm for solving the discretized modified equations. In this section, we

consider the standard model problems to show that the multigrid part of $R_M T$ is independent of problems to be solved.

Let us consider a boundary value problem

$$\frac{\partial}{\partial x}\left(\lambda^x(x,y)\,\frac{\partial U}{\partial x}\right)+\frac{\partial}{\partial y}\left(\lambda^y(x,y)\,\frac{\partial U}{\partial y}\right)+\gamma(x,y)\,U+F(x,y)=0\,,\qquad U\big|_{\partial\Omega}=g \tag{16}$$

in $\Omega=(0,1)\times(0,1)$. The Σ-modification of its solution $U(x,y)=C(x,y)+\hat{U}(x,y)$ leads to the following Σ-modified form of (16):

$$\frac{\partial}{\partial x}\left(\lambda^x(x,y)\,\frac{\partial C}{\partial x}\right)+\frac{\partial}{\partial y}\left(\lambda^y(x,y)\,\frac{\partial C}{\partial y}\right)+\gamma(x,y)\,C=r(x,y)\,,\qquad C\big|_{\partial\Omega}=g-\hat{U}\big|_{\partial\Omega}$$

Here

$$r(x,y)=-F(x,y)-\gamma(x,y)\,\hat{U}-\frac{\partial}{\partial x}\left(\lambda^x(x,y)\,\frac{\partial\hat{U}}{\partial x}\right)-\frac{\partial}{\partial y}\left(\lambda^y(x,y)\,\frac{\partial\hat{U}}{\partial y}\right)$$

Assume that a uniform computational grid ($\Delta=H_0{}^{-1}$) and the multigrid structure have been generated, and that the functions C and $\hat{U}$ are assigned to grid points $(x^{\rm v},y^{\rm v})$. Integration of the Σ-modified equation over control volume (10) yields the following finite-difference scheme:

$$\begin{aligned}&\Gamma^x_{\{ij\}}\frac{C_{\{i+1j\}}-C_{\{ij\}}}{\Delta^2\,3^{2L}}-\Gamma^x_{\{i-1j\}}\frac{C_{\{ij\}}-C_{\{i-1j\}}}{\Delta^2\,3^{2L}}\\ +&\Gamma^y_{\{ij\}}\frac{C_{\{ij+1\}}-C_{\{ij\}}}{\Delta^2\,3^{2L}}-\Gamma^y_{\{ij-1\}}\frac{C_{\{ij\}}-C_{\{ij-1\}}}{\Delta^2\,3^{2L}}+\langle\gamma\rangle_{\{ij\}}\,C_{\{ij\}}=J_{\{ij\}}\end{aligned} \tag{17}$$

Here

$$\Gamma^x_{\{ij\}}=\frac{1}{\Delta 3^L}\int\limits_{y^{\rm f}_{\{j-1\}}}^{y^{\rm f}_{\{j\}}}\lambda^x\left(x^{\rm f}_{\{i\}},y\right)\,dy\,,\qquad \Gamma^y_{\{ij\}}=\frac{1}{\Delta 3^L}\int\limits_{x^{\rm f}_{\{i-1\}}}^{x^{\rm f}_{\{i\}}}\lambda^y\left(x,y^{\rm f}_{\{j\}}\right)\,dx \tag{18}$$

are the averaged values of the coefficients $\lambda^x(x,y)$ and $\lambda^y(x,y)$ along the boundaries of the control volume. The coefficients $\langle\gamma\rangle$ given by (11) are the integral mean values of the function $\gamma(x,y)$ over the control volume. The integral J on the finest grid is computed as follows:

$$\begin{aligned}R^\star_{mk}=&-F_{mk}-\langle\gamma\rangle_{mk}\,\hat{U}_{mk}-\Gamma^x_{mk}\frac{\hat{U}_{m+1k}-\hat{U}_{mk}}{\Delta^2}-\Gamma^x_{m-1k}\frac{\hat{U}_{mk}-\hat{U}_{m-1k}}{\Delta^2}\\ &-\Gamma^y_{mk}\frac{\hat{U}_{mk+1}-\hat{U}_{mk}}{\Delta^2}-\Gamma^y_{mk-1}\frac{\hat{U}_{mk}-\hat{U}_{mk-1}}{\Delta^2}+o(\Delta^2)\end{aligned} \tag{19}$$

In general, the integrals Γ^x, Γ^y, J and the coefficients $\langle\gamma\rangle$ should be computed on the finest grid with an accuracy of $o(\Delta^2)$ to obtain the extremely accurate formulation of the discrete problems on the coarse grids (Section 5). In our numerical tests, it is accepted that:

1) the exact solution of a model problem is $U_e(x,y)=f(x)f(y)$, where the function f is defined by (2). The function F is obtained by substitution of the exact solution into (16). In this case, $g=0$;

2) a starting guess is taken to be zero: $U^0(x,y)=0$;

3) error of the numerical solution is defined as $E=\max_{ij}|\,U_e(x^{\rm v}_i,y^{\rm v}_j)-U_{ij}|$;

4) three smoothing iterations are performed on finer levels: $\nu=3\,,\ 0\leqslant L<L^+$.

7.1. The isotropic equation. ($\lambda^x=\lambda^y=1$; $\gamma=0$) For given λ^x, λ^y and γ, we have from (18) that $\Gamma^x_{\{ij\}}=\Gamma^y_{\{ij\}}=1$ and $\langle\gamma\rangle_{\{ij\}}=0$. Two tests were performed as a numerical experiment:

Test 1: The five-point discretization of the Poisson equation ((17)–(19))

$$\begin{aligned}&\frac{C_{\{i-1j\}}-2C_{\{ij\}}+C_{\{i+1j\}}}{\Delta^2\,3^{2L}}+\frac{C_{\{ij-1\}}-2C_{\{ij\}}+C_{\{ij+1\}}}{\Delta^2\,3^{2L}}=J_{\{ij\}}\\ &R^\star_{mk}=-F_{mk}-\frac{\hat{U}_{m-1k}-2\hat{U}_{mk}+\hat{U}_{m+1k}}{\Delta^2}-\frac{\hat{U}_{mk-1}-2\hat{U}_{mk}+\hat{U}_{mk+1}}{\Delta^2}+o(\Delta^2)\end{aligned}$$

Test 2: The (five+nine)-point discretization of the Poisson equation. Unfortunately, the high-order accuracy cannot be obtained directly on the multigrid structure. Accuracy of the numerical solution depends strongly

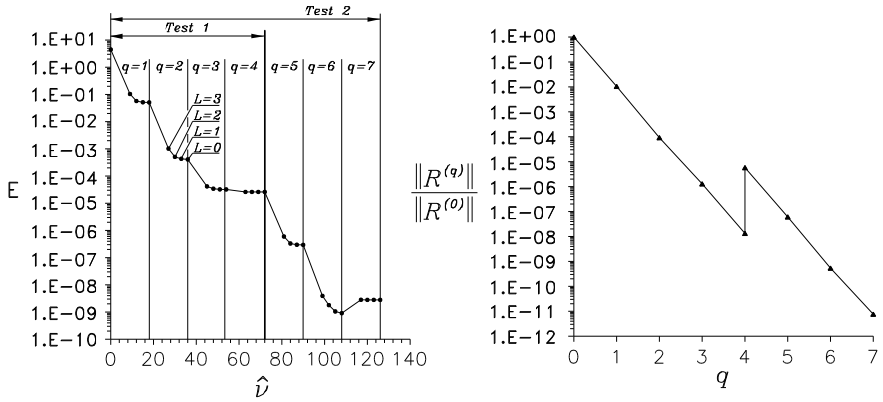

Fig. 7. Convergence behavior in the first and second tests on the finest 111×111 grid

Table 4. Multigrid convergence in the first test

Finest Grid	L^+	$\hat{\nu}_\Sigma$	q	ρ_q	$\rho_{\hat{\nu}}$	E
16×16	1	56	4	0.012	0.726	$1.66 \cdot 10^{-3}$
41×41	2	60	4	0.013	0.747	$2.34 \cdot 10^{-4}$
111×111	3	64	4	0.011	0.754	$3.09 \cdot 10^{-5}$
351×351	4	80	4	0.014	0.806	$3.08 \cdot 10^{-6}$
1001×1001	5	89	4	0.029	0.852	$3.90 \cdot 10^{-7}$

on the approximation of the boundary conditions on coarse grids ((6)–(9)). The five-point discretization of the left-hand side differential operator and the nine-point discretization of the right-hand side integrals $R^\star$ yield a more accurate solution. Assume that the solution of second order accuracy has been obtained (Test 1). To obtain the solution of fourth order accuracy, the integrals $R^\star$ must be computed as

$$R^\star_{mk} = -F_{mk} + \frac{\Delta^2}{12}\left(\frac{\partial^2 F}{\partial x^2} + \frac{\partial^2 F}{\partial y^2}\right)_{mk} - \frac{1}{6\Delta^2}\begin{pmatrix} \hat{U}_{m-1k+1} + & 4\hat{U}_{mk+1} + & \hat{U}_{m+1k+1} \\ +\,4\hat{U}_{m-1k} & -\,20\hat{U}_{mk} & +\,4\hat{U}_{m+1k} \\ +\ \hat{U}_{m-1k-1} + & 4\hat{U}_{mk-1} + & \hat{U}_{m+1k-1} \end{pmatrix} + o(\Delta^4)$$

The convergence behavior in the first and second tests is shown in Figure 7. The average reduction factors ρ_q and $\rho_{\hat{\nu}}$ are defined as

$$\rho_q = \left(\frac{\|R^{(q)}\|}{\|R^{(0)}\|}\right)^{1/q} \qquad \text{and} \qquad \rho_{\hat{\nu}} = \left(\frac{\|R^{(\hat{\nu})}\|}{\|R^{(0)}\|}\right)^{1/\hat{\nu}}$$

where $\|\cdot\|$ is the l_2-norm, R is the residual on the finest grid, $R^{(0)}$ is the initial residual, and q is the number of the multigrid iterations. Table 4 represents the average reduction factors as a function of mesh size in the first test.

Note that the average reduction factor ρ_q does not allow us to make accurate comparison between CMM and RMT. Generally, this factor can be used only to estimate the efficiency of different variants of CMM. A more accurate comparison should consider the reduction factor $\rho_{\hat{\nu}}$ as a function of computational efforts. Experimentally, for the Poisson equation, RMT achieves a reduction of the residual by a factor of 0.01–0.03 per multigrid iteration. This is in contrast to a factor of 0.125–0.250 for CMM [9]. On the other hand, there is a penalty for RMT in the computational efforts (Section 8).

7.2. The anisotropic equation. ($\lambda^x \gg \lambda^y$ or $\lambda^x \ll \lambda^y$; $\gamma = -0.25$) Following Hackbusch [1], consider the boundary value problem

$$\lambda^x \frac{\partial^2 U}{\partial x^2} + \lambda^y \frac{\partial^2 U}{\partial y^2} - \frac{1}{4}U + F(x,y) = 0\,, \qquad \lambda^x, \lambda^y > 0$$

in $\Omega = (0,1) \times (0,1)$.

Test 3: The five-point discretization; uniform 151×151 finest grid ($L^+ = 3$). In this case, $\Gamma^x_{\{ij\}} = \lambda^x$, $\Gamma^y_{\{ij\}} = \lambda^y$, and $\langle\gamma\rangle_{\{ij\}} = -0.25$. Table 5 represents the average reduction factor of the residual ρ_q as a function of λ^x and λ^y.

Table 5. Multigrid convergence (ρ_q) in the third test

$\lambda^x \setminus \lambda^y$	10^{-3}	10^{-2}	10^{-1}	10^{+0}	10^{+1}	10^{+2}	10^{+3}
10^{-3}	0.003	0.038	0.035	0.002	0.000	0.000	0.000
10^{-2}	0.038	0.008	0.101	0.039	0.002	0.000	0.000
10^{-1}	0.035	0.101	0.010	0.125	0.040	0.002	0.000
10^{+0}	0.002	0.039	0.125	0.010	0.125	0.040	0.002
10^{+1}	0.000	0.002	0.040	0.125	0.010	0.125	0.040
10^{+2}	0.000	0.000	0.002	0.040	0.125	0.010	0.127
10^{+3}	0.000	0.000	0.000	0.002	0.040	0.127	0.010

Theoretical analysis shows that ALGS is a robust smoother for the anisotropic diffusion equation [2], but the most powerful coarse grid correction strategy in RMT makes it possible to avoid the necessity of line smoothers for anisotropic problems.

7.3. Discontinuous coefficients. Discontinuous coefficients requires special treatment in the CMM context. Much has been written in the CMM literature about the pros and cons of various prolongations in different classical multigrid algorithms [2]. We will not go into this here.

RMT does not require any sophisticated implementations of the transfer operators for different problems. Assume that the discontinuities of the coefficient $\lambda^x(x,y)$ lie at boundaries of control volumes (Figure 8). In this case, the coefficient $\Gamma^x_{\{ij\}}$ in (17) is defined as

$$\Gamma^x_{\{ij\}} = \frac{\hat\Gamma^x_{\{ij\}}\hat\Gamma^x_{\{i+1j\}}}{(1-\zeta)\,\hat\Gamma^x_{\{ij\}} + \zeta\,\hat\Gamma^x_{\{i+1j\}}}\,, \qquad \zeta = \frac{x^* - x^{\mathrm{v}}_{\{i\}}}{\Delta 3^L} \in (0,1)$$

where

$$\hat\Gamma^x_{\{ij\}} = \frac{1}{\Delta 3^L}\int\limits_{y^{\mathrm{f}}_{\{j-1\}}}^{y^{\mathrm{f}}_{\{j\}}} \lambda^x(x^{\mathrm{v}}_{\{i\}}, y)\,dy$$

When the discontinuity of $\lambda^x(x,y)$ is located between the grid points $x^{\mathrm{v}}_{\{i\}}$ and $x^{\mathrm{v}}_{\{i+1\}}$, we obtain

$$x^* - x^{\mathrm{v}}_{\{i\}} = x^{\mathrm{v}}_{\{i+1\}} - x^* \Rightarrow \zeta = 0.5 \Rightarrow \Gamma^x_{\{ij\}} = \frac{2\hat\Gamma^x_{\{ij\}}\hat\Gamma^x_{\{i+1j\}}}{\hat\Gamma^x_{\{ij\}} + \hat\Gamma^x_{\{i+1j\}}}$$

where $\Gamma^x_{\{ij\}}$ is the harmonic averaged value of $\hat\Gamma^x_{\{ij\}}$ and $\hat\Gamma^x_{\{i+1j\}}$ [2, 4, 10].

Following Wessiling [10], consider the model problem (Figure 8)

$$\frac{\partial}{\partial x}\left(\lambda^x(x,y)\,\frac{\partial U}{\partial x}\right) + \frac{\partial}{\partial y}\left(\lambda^y(x,y)\,\frac{\partial U}{\partial y}\right) + xy = 0\,, \qquad U\big|_{\partial\Omega} = x^2 + y^2$$

Test 4: The five-point discretization; uniform 151×151 finest grid ($L^+ = 3$); $\lambda_e = 1$. Table 6 represents the average reduction factor of the residual ρ_q as a function of λ_i.

Comparing the rate of convergence that are reported one gets the impression that RMT is at least as efficient as CMM.

7.4. Nonlinear equations. In recent years, several classical multigrid algorithms for solving nonlinear problems have been proposed and developed [2]. The absence of pre-smoothing in RMT impressively simplifies nonlinear robust iterations. To illustrate a formal application of RMT to some nonlinear problems, consider the following model problem:

$$\frac{\partial^2 U}{\partial x^2} + \frac{\partial^2 U}{\partial y^2} - \alpha U^2 + F(x,y) = 0\,, \qquad U\big|_{\partial\Omega} = 0\,, \qquad \alpha > 0 \tag{20}$$

The function F is chosen so that the solution is $U_e(x,y) = f(x)f(y)$, where f is defined by (2). Equation (20) may be rewritten in the Σ-modified form as

$$\frac{\partial^2 C}{\partial x^2} + \frac{\partial^2 C}{\partial y^2} - \alpha(C^2 + 2C\hat U) = r(x,y), \qquad r(x,y) = -F(x,y) - \frac{\partial^2 \hat U}{\partial x^2} - \frac{\partial^2 \hat U}{\partial x^2} + \alpha \hat U^2$$

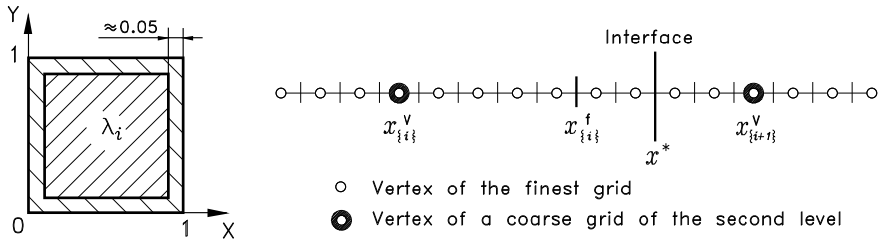

Fig. 8. Geometry of the model problem and location of an interface

Table 6. Multigrid convergence in the fourth test

λ_i	10^0	10^1	10^2	10^3	10^4	10^5	10^6
ρ_q	0.016	0.064	0.106	0.123	0.144	0.170	0.188

Assume that a uniform finest grid ($\Delta = \mathrm{H_0}^{-1}$) has been generated and the function U is assigned to the grid points $(x^{\mathrm{v}}, y^{\mathrm{v}})$. Integration of the Σ-modified equations over a control volume yields the following finite-difference scheme

$$\mathcal{L}_{\{ij\}}(C) - \alpha(C^2_{\{ij\}} + 2C_{\{ij\}}\langle\hat{U}\rangle_{\{ij\}}) = J_{\{ij\}}$$

Here $\mathcal{L}_{\{ij\}}$ is the standard five-point representation of Laplacian and

$$\Theta_{\{ij\}} = \frac{1}{\Delta^2\, 3^{2L}} \int\limits_{x^{\mathrm{f}}_{\{i-1\}}}^{x^{\mathrm{f}}_{\{i\}}} \int\limits_{y^{\mathrm{f}}_{\{j-1\}}}^{y^{\mathrm{f}}_{\{j\}}} \theta(x,y)\, dy\, dx\,, \qquad \Theta = \begin{pmatrix} \langle\hat{U}\rangle \\ J \end{pmatrix}\,, \quad \theta = \begin{pmatrix} \hat{U} \\ r \end{pmatrix}$$

and the integral J can be computed on the finest grid ($L = 0$) as follows

$$R^{\star}_{mk} = -F_{mk} - \mathcal{L}_{mk}(\hat{U}) + \alpha\hat{U}^2_{mk} + o(\Delta^2)\,, \qquad \langle\hat{U}\rangle_{mk} = \hat{U}_{mk} + o(\Delta^2)$$

It is necessary to remember that the integrals J and $\langle\hat{U}\rangle$ are computed on the finest grid with the approximation order $o(\Delta^2)$ to obtain the extremely accurate formulation of the discrete problems on coarse grids. The nonlinear Σ-modified problem can be linearized and solved iteratively on each grid of the multigrid structure, for example, by Newton–Raphson's method. This works well as long as the Jacobian of the nonlinear discrete problems is nonsingular. The nonlinear $\mathrm{R_M T}$ can be used efficiently, because the global system is not linearized.

Test 5: Uniform 361×361 finest grid ($L^+ = 4$). Table 7 represents the average reduction factor of the residual ρ_q and the error E as a functions of parameter α. Of course, computation of $\langle\hat{U}\rangle$ increases the computational efforts per robust multigrid iteration approximately by

$$\frac{2\cdot 3^N + 4(N-1)N\nu}{3^N + 4(N-1)N\nu} = 1.27$$

times (LMC at $\nu = 3$) as compared with $\alpha \equiv 0$.

It should be noted that the Π-modification $U = C\hat{U}$ of some nonlinear equation

$$\hat{U}^{(q)} = \begin{cases} 1\,, & q = 1 \\ \hat{U}^{(q-1)}C^{(q-1)}\,, & q > 1 \end{cases}$$

Table 7. Multigrid convergence in the fifth test

α	10^{-3}	10^{-2}	10^{-1}	10^{+0}	10^{+1}
ρ_q	0.015	0.015	0.014	0.012	0.008
E	$2.91\cdot10^{-6}$	$2.90\cdot10^{-6}$	$2.81\cdot10^{-6}$	$2.09\cdot10^{-6}$	$5.81\cdot10^{-7}$

may be more preferable than the Σ-modification. For example, the ε-equation of the Launder–Sharma model [11] may be written as

$$\frac{\partial(\rho u\varepsilon)}{\partial x}+\frac{\partial(\rho v\varepsilon)}{\partial y}=\frac{\partial}{\partial x}\left(\mu_e\frac{\partial\varepsilon}{\partial x}\right)+\frac{\partial}{\partial y}\left(\mu_e\frac{\partial\varepsilon}{\partial y}\right)+A\frac{\varepsilon}{k}-B\frac{\varepsilon^2}{k}+E$$

where

$$\mu_e=\mu+\frac{\mu_t}{\sigma_\varepsilon},\qquad A=C_{\varepsilon 1}f_1\mu_t\left(\left(\frac{\partial u}{\partial x}\right)^2+\left(\frac{\partial u}{\partial y}\right)^2\right),\qquad B=C_{\varepsilon 2}f_2\rho,\qquad E=2\,\frac{\mu\mu_t}{\rho}\left(\frac{\partial^2 u}{\partial y^2}\right)^2$$

The Π-modified form of the ε-equation ($\varepsilon=c_\varepsilon\hat{\varepsilon}$ and $K=c_k\hat{k}$) is given by

$$\frac{\partial(\rho u^* c_\varepsilon)}{\partial x}+\frac{\partial(\rho v^* c_\varepsilon)}{\partial y}=\frac{\partial}{\partial x}\left(\mu_e^*\frac{\partial c_\varepsilon}{\partial x}\right)+\frac{\partial}{\partial y}\left(\mu_e^*\frac{\partial c_\varepsilon}{\partial y}\right)+A^*\frac{c_\varepsilon}{c_k}-B^*\frac{(c_\varepsilon)^2}{c_k}+E$$

where

$$A^*=A\,\frac{\hat{\varepsilon}}{\hat{k}},\qquad B^*=B\,\frac{\hat{\varepsilon}^2}{\hat{k}},\qquad \mu_e^*=\mu_e\hat{\varepsilon},\qquad u^*=u\hat{\varepsilon}-\frac{\mu_e}{\rho}\,\frac{\partial\hat{\varepsilon}}{\partial x},\qquad v^*=v\hat{\varepsilon}-\frac{\mu_e}{\rho}\,\frac{\partial\hat{\varepsilon}}{\partial y}$$

The Π-modification does not change the form of the ε-equation.

8. Robustness versus efficiency. The dilemma of robustness versus efficiency appears in various fields of numerical mathematics [2]. R$_{\rm M}$T requires the least number of iterations to obtain a numerical solution; however, computational cost of the iterations is high enough. Therefore, C$_{\rm M}$M can be more efficient for solving the simplest problems than R$_{\rm M}$T. On the other hand, C$_{\rm M}$M can be an inefficient solver for the complicated problems, which can be solved effectively by R$_{\rm M}$T. In general, comparison between C$_{\rm M}$M and R$_{\rm M}$T is problem-dependent.

Let us estimate a maximum penalty in computational efforts for R$_{\rm M}$T. Assume that some problem (for example, the Poisson equation) can be solved efficiently by C$_{\rm M}$M (the multigrid schedule is V-cycle, the smoother is ALGS, the cost of the transfer operators is $C_T\bar{\mathbf{N}}$ f.p.o.). The cost of each classical iteration can be estimated as

$$\big(8(N-1)N\nu+C_T\big)\bar{\mathbf{N}}\left(2\sum_{l=0}^{L^+}2^{-Nl}-1\right)\approx\big(8(N-1)N\nu+C_T\big)\bar{\mathbf{N}}\frac{2^N+1}{2^N-1}$$

The cost of each robust iteration (LMC) can be estimated as

$$\big(8(N-1)N\nu+C_I\big)\frac{\bar{\mathbf{N}}\lg\bar{\mathbf{N}}}{N\lg 3}\approx\big(8(N-1)N\nu+C_I\big)\frac{2}{N}\,\bar{\mathbf{N}}\lg\bar{\mathbf{N}}$$

The ratio of total computational efforts takes the form

$$\frac{q_\Sigma^c}{q_\Sigma^r}\,\frac{2^N+1}{2^N-1}\,\frac{N}{2}\,\frac{8(N-1)N\nu+C_T}{8(N-1)N\nu+C_I}\,\frac{1}{\lg\bar{\mathbf{N}}}$$

where q_Σ^c and q_Σ^r are the numbers of classical and robust iterations, respectively. Assuming that $q_\Sigma^c=2q_\Sigma^r$ and $8(N-1)N\nu\gg\max(C_T,C_I)$, we obtain

$$\frac{\text{total efforts in C}_{\rm M}\text{M}}{\text{total efforts in R}_{\rm M}\text{T}}\;\approx\;\frac{2^N+1}{2^N-1}\,\frac{N}{\lg\bar{\mathbf{N}}}$$

This estimate shows that there is no drastic penalty for R$_{\rm M}$T in computational work (Table 8). From the practical point of view, for very simple problems the computational time for C$_{\rm M}$M is several times less than it for R$_{\rm M}$T. This is an unavoidable penalty for the expanded robustness.

Acknowledgments. The author is indebted to R. P. Fedorenko for his valuable comments. We also thank the referees for a very critical reading of the manuscript which resulted in a few corrections and impressive improvements in the exposition.

9. Conclusion. Very simple PDEs are solved for demonstration of robustness and efficiency of R$_{\rm M}$T. All model problems require only a single Σ-modification for their adaption to R$_{\rm M}$T. Consequently, the next step in the development of R$_{\rm M}$T will be the systematic investigation of methods for adaption of PDEs to this technique, since the other components of R$_{\rm M}$T are problem-independent.

Table 8. Estimation of the ratio of total efforts ($C_M M$ vs $R_M T$)

the number of grid points ($\bar{N}$)	10^4	10^5	10^6	10^7	10^8	10^9
2D problems	0.83	0.67	0.56	0.48	0.42	0.37
3D problems	0.96	0.77	0.64	0.55	0.48	0.43

REFERENCES

1. W. Hackbusch, "Robust multi-grid methods, the frequency decomposition multi-grid algorithm, in: *Notes on Numerical Fluid Mechanics*, Volume 23, pp. 96–104, Braunschweig, 1989.
2. P. Wesseling, *An Introduction to Multigrid Methods*, Chichester, 1991.
3. R.P. Fedorenko, "The rate of convergence of one iterative process", *USSR Comput. Math. and Math. Phys.*, **4**, 3: 227–235, 1964.
4. S. Patankar, *Numerical Heat Transfer and Fluid Flow*, New York, 1980.
5. B. Koren, "Defect correction and multigrid for an efficient and accurate computation of airfoil flows", *J. Comput. Phys.*, **77**: 183–206, 1988.
6. W. Hackbusch, *Multi-grid Methods and Applications*, Berlin, 1985.
7. S.I. Martynenko, "Template for the solution of partial differential equations: building blocks and diagnostic tools for the robust multigrid technique", *Numerical Methods and Programming*, (to appear).
8. A. Brandt, "Multi-level adaptive solutions to boundary value problems", *Math. Comput.*, **31**: 333–390, 1977.
9. J. E. Dendy, "Black box multigrid", *J. Comput. Phys.*, **48**: 366–386, 1982.
10. P. Wessiling, "Cell-centered multigrid for interface problem", *J. Comput. Phys.*, **79**: 85–91, 1988.
11. B. Launder and B. Sharma, "Application of the energy dissipation model of turbulence to the calculation of flow near a spinning disc", *Letters in Heat and Mass Transfer*, **1**: 131–138, 1974.

16 October 2000